International Journal of Advanced Robotic Systems

OPEN ACCESS ARTICLE

Robust Adaptive Control of a Free-floating Space Robot System in Cartesian Space

Regular Paper

Fuhai Zhang[1]*, Yili Fu[1]*, Jiadi Qu[1] and Shuguo Wang[1]

1 State Key Laboratory of Robotics and System, Harbin Institute of Technology, Harbin, Heilongjiang, China
*Corresponding author(s) E-mail: zfhhit@hit.edu.cn; meylfu_hit@163.com

Received 13 April 2015; Accepted 11 October 2015

DOI: 10.5772/61743

Abstract

This paper presents a novel, robust, adaptive trajectory-tracking control scheme for the free-floating space robot system in Cartesian space. The dynamic equation of the free-floating space robot system in Cartesian space is derived from the augmented variable method. The proposed basic robust adaptive controller is able to deal with parametric and non-parametric uncertainties simultaneously. Another advantage of the control scheme is that the known and unknown external disturbance bounds can be considered using a modification of the parameter-estimation law. In addition, three cases are certified to achieve robustness for both parametric uncertainties and external disturbances. The simulation results show that the control scheme can ensure stable tracking of the desired trajectory of the end-effector.

Keywords Free-floating Space Robot, Cartesian Space, Robust Adaptive Control, Parametric Uncertainty, Non-parametric Uncertainty

1. Introduction

Space has attracted special interest as a new application field of robotics. The space manipulator system composed of the satellite as the base and the manipulators attached to the satellite has wide applications in assembly of the space station, and in complicated and dangerous space missions such as the capture and on-orbit services of the space target. The pose-controlled base has a pose-control system, such as reaction wheels and jet propellers, which could counteract the influence of the manipulator movement on the base pose. However, the reaction wheels tend to be saturated, and the jet propellers consume the limited and irreproducible chemical fuel, which will reduce the lifetime of the satellite. In order to conserve the precious fuel carried by the base, neither the position nor the attitude of the base should be controlled. The base is allowed to translate and rotate freely in response to manipulator motions. This system is called a free-floating space robot (FFSR) system. In an environment with microgravity, it is inevitable that the unfixed pose of the base leads to a coupling effect between the manipulator and the base, making the dynamics and control of the FFSR system more challenging than those of ground manipulators with fixed bases [1-3].

An FFSR system has non-holonomic characteristics due to the non-integrability of the angular momentum. Many researchers have focused on kinematics, dynamics and control problems of the FFSR system. Umetani and Yoshida derived the general Jacobian matrix (GJM), which is of great use in the control of space robots; GJM is used not only successfully in the resolved motion rate control (RMRC) of space robots, but also in resolved motion acceleration control (RMAC) and the transposed

Jacobian matrix control of space robots [4, 5]. However, the method is essentially part of the inverse kinematics without adaptation and robustness, and cannot deal with the uncertainties of dynamic parameters existing in GJM. Some system parameters cannot be determined accurately in an actual FFSR system, for example, the component mass, the position of the centre of mass and the moment of inertia cannot be determined due to the complicated structure of the manipulator system. In addition, when the target of the space robot is disabled satellites, maintenance tools, etc., the system parameters are unknown. Thus, the space robot should possess the capability whereby the end-effector of the manipulator can track the desired trajectory stably, despite parametric uncertainties [6, 7]. Walker and Xu designed the adaptive control scheme aiming at the uncertainty existence of mass and inertial parameters of a space manipulator with a controlled base attitude, which could ensure the stable tracking of a desired trajectory and a desired base attitude of a manipulator in joint space [8, 9]. However, the aforementioned controlled research projects of space robots all aim at the condition of a controlled base attitude and cannot ensure the controller's effectiveness in an FFSR system with an uncontrolled base attitude and position. These differences confront the FFSR control with two basic difficulties. One is that the dynamic coupling causes the Jacobian matrix to be related not only to geometrical parameters but also to dynamic parameters such as mass, the moment of inertia, etc.; thus, the Jacobian matrix cannot be determined due to the uncertainties of dynamic parameters, which may lead to a situation in which the reference trajectory in Cartesian space cannot be realized in joint space. The other problem is that the system-dynamic equation cannot be linearly parameterized; thus, most of the adaptive and non-linear control schemes for the robots with ground-fixed bases cannot work within the FFSR system. To overcome the circumstance in which the dynamic equation cannot be linearly parameterized and uncertainties exist in the system, Gu et al. put forward the extended manipulator-model method, formed the augmented variable by combining the parameters of the end effector and joints (which linearized the inertial parameters of the system-dynamic equation) and obtained the system control law and parameter-estimation law by introducing an intermediate variable and the constructed Lyapunov function [10]. The method could ensure stable tracking of the manipulator's end effector to the desired trajectory in Cartesian space, but the controller required that the base position, velocity and acceleration were measurable. Parlaktuna et al. put forward an online adaptive control scheme in Cartesian space, but the controller parameters designed by the scheme were all obtained via online estimation, hence the scheme was not suitable for real-time control because the complexity of the dynamic equation of the FFSR system led to a large amount of computation [11, 12].

The self-tuning control method, i.e., indirect adaptive control, can identify system parameters online using a parameter estimator then translating the estimated parameters into controller parameters. Thus, it is very effective when the model parameters are uncertain, but non-parameterized uncertainties such as external disturbances may exist in the real system. If the controller does not consider the non-parameterized uncertainties, the adaptive controller cannot ensure the stability of the system [13, 14]. The robust control can restrain the uncertain elements within a limited range, ensure the system's stability and maintain a certain performance index [15]. Shin [16] proposed a robust, adaptive trajectory-tracking control method aiming at the parametric uncertainty and external disturbance existing in the FFSR system, and used the adaptive law to online estimate the upper bounds of the uncertainty; the method, however, did not analyse the restraint performance of the control system regarding the external disturbance.

Aiming at the existence of unmodelled dynamics and external disturbance of the FFSR system, Feng et al. designed a robust adaptive controller in Cartesian space using the Lyapunov law and dissipative theory [17]. Chu et al. designed a robust control scheme for the FFSR system based on a disturbance observer [18]. They divided the dynamic model into an inertial item and a disturbance item, in such a way that the inertial item could be separated linearly and the computation efficiency of the method was high. An indirect adaptive control strategy was proposed based on the extended manipulator model, but the parameters of the controller needed to be obtained via online calculations, which increased the calculation burden and could not guarantee the reversibility of the inertial matrix [19]. Other scholars [20-23] studied the adaptive control issue of the FFSR system using fuzzy or neural network theories, but these were approximations of the mathematical model of the system, which had errors when compared with the actual model of the system.

A robust, adaptive trajectory-tracking control method in Cartesian space is proposed in the paper. The dynamic equations of the FFSR system in Cartesian space are derived from the augmented variable method. A basic robust, adaptive trajectory-tracking control method is studied, and the system's robust stability is proven. A robust, adaptive trajectory-tracking control method that considers the known or unknown factors of bounded disturbances' forms was designed just by modifying the parameter-estimation law. The simulation results show that the control scheme can ensure stable tracking of the end-effector's desired trajectory.

2. Dynamic model in Cartesian space

2.1 Model assumption

The FFSR system in the inertial coordinates is set up as in Fig.1. The meanings of the symbols in Fig.1 are as follows: O_{cm} represents the mass centre of the system; O_b represents

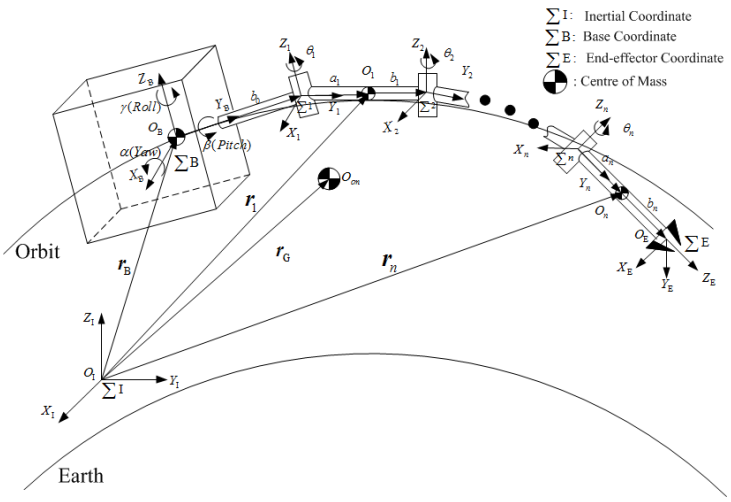

Figure 1. The FFSR system

the mass centre of the base; O_i represents the mass centre of the link i; $\boldsymbol{r}_B$ represents the position vector of the mass centre of the base in the inertial coordinates; $\boldsymbol{r}_G$ represents the position vector of the mass centre of the system in the inertial coordinates; $\boldsymbol{r}_i$ represents the position vector of the mass centre of link i in the inertial coordinates; a_i represents the distance between joint i and the mass centre O_i of link i; b_i represents the distance between the mass centre O_i of link i and joint i+1; α, β, γ represents the attitude angles of the base (yaw, pitch, roll) and θ_i represents the rotation angle of the joint i (i=0, 1, 2, ⋯, n).

2.2 Dynamic model with external disturbances in Cartesian space

Because of the non-linearity of the dynamic equation, which is caused by the dynamic coupling effect between the manipulator and the base in the FFSR system, the extended manipulator method is adopted. The base of the FFSR is treated as a virtual manipulator with six degrees of freedom (DOF), including three rotational DOFs and three translational DOFs, and the virtual manipulator (together with the real manipulator with n joints) can compose a new manipulator with m=n+6 DOFs — namely, the extended manipulator [10]. Thus, the system-dynamic equation in joint space can be obtained using the methods similar to those used for the fixed-base robots. If the influence of gravity is ignored, then the Lagrange equation based on the extended manipulator model is:

$$\frac{d}{dt}\frac{\partial L}{\partial \dot{\boldsymbol{\Theta}}} - \frac{\partial L}{\partial \boldsymbol{\Theta}} = \boldsymbol{\tau}_a, \tag{1}$$

where L is the Lagrange function; L=T-P, T is the kinetic energy; P is the potential energy; $\boldsymbol{\tau}_a$ is the general torque of the extended manipulator; $\boldsymbol{\tau}_a$=$(\boldsymbol{0} \quad \boldsymbol{\tau})^{\mathrm{T}}$, $\boldsymbol{\tau}$ is the torque exerted on the real manipulator joint; $\boldsymbol{\tau} \in \Re^n$; $\boldsymbol{\Theta}$ is the general translation vector of the joint; $\boldsymbol{\Theta}$=$(\boldsymbol{\Theta}_s^{\mathrm{T}} \quad \boldsymbol{\Theta}_m^{\mathrm{T}})^{\mathrm{T}}$, $\boldsymbol{\Theta}_s$ is the general translation vector of the base (pseudo manipulator) joint and $\boldsymbol{\Theta}_s \in \Re^6$, $\boldsymbol{\Theta}_m$ is the general translation vector of the real manipulator with n joints, $\boldsymbol{\Theta}_m \in \Re^n$.

From (1), the dynamic equation of the FFSR system in joint space can be obtained and linearized as:

$$\boldsymbol{\Omega}(\boldsymbol{\Theta})\ddot{\boldsymbol{\Theta}} + \boldsymbol{K}(\boldsymbol{\Theta},\dot{\boldsymbol{\Theta}})\dot{\boldsymbol{\Theta}} = \begin{pmatrix} \boldsymbol{0} \\ \boldsymbol{\tau} \end{pmatrix} = \boldsymbol{\tau}_a = \boldsymbol{W}_a(\boldsymbol{\Theta},\dot{\boldsymbol{\Theta}},\ddot{\boldsymbol{\Theta}})\boldsymbol{\alpha}, \tag{2}$$

where $\boldsymbol{\Omega}(\boldsymbol{\Theta}) \in R^{m\times m}$ is the system inertial matrix that is symmetrically positive definite; $\boldsymbol{K}(\boldsymbol{\Theta}, \dot{\boldsymbol{\Theta}}) \in R^{m\times m}$ is the system centrifugal force and Coriolis force; $\boldsymbol{W}_a(\boldsymbol{\Theta}, \dot{\boldsymbol{\Theta}}, \ddot{\boldsymbol{\Theta}}) \in R^{m\times r}$ is the regression matrix, which is composed of non-linear functions related to geometrical parameters and kinematics data and $\boldsymbol{\alpha} \in R^r$ is the vector of separated, unknown inertial parameters or their combination.

Besides the parametric uncertainties, non-parametric uncertainties may also exist in the actual system, such as the uncertainty caused by friction due to the manipulator's slow movement and the contact caused by the manipulator grasping the load, the effect of which equals the external-disturbance torque exerted on the system. This paper considers the external disturbances exerted on the manipulator and the base simultaneously, and treats them as the external-disturbance torques exerted on the system. Therefore, the dynamic model in the joint space of the FFSR system is:

$$\boldsymbol{\Omega}(\boldsymbol{\Theta})\ddot{\boldsymbol{\Theta}} + \boldsymbol{K}(\boldsymbol{\Theta},\dot{\boldsymbol{\Theta}})\dot{\boldsymbol{\Theta}} = \begin{pmatrix} \boldsymbol{D}_s \\ \boldsymbol{\tau} + \boldsymbol{D}_m \end{pmatrix}, \tag{3}$$

where $\boldsymbol{D}_s \in R^6$ is the external disturbance exerted on the base and $\boldsymbol{D}_m \in R^n$ is the external disturbance exerted on the manipulator.

Taking the time derivative of the system output augmentation to be $\boldsymbol{X}=\begin{pmatrix}\boldsymbol{x}\\ \boldsymbol{\Theta}_s\end{pmatrix}\in\boldsymbol{R}^m$, we have:

$$\dot{\boldsymbol{X}}=\begin{pmatrix}\dot{\boldsymbol{x}}\\ \dot{\boldsymbol{\Theta}}_s\end{pmatrix}=\begin{pmatrix}\boldsymbol{J}_s & \boldsymbol{J}_m\\ \boldsymbol{I} & \boldsymbol{O}\end{pmatrix}\begin{pmatrix}\dot{\boldsymbol{\Theta}}_s\\ \dot{\boldsymbol{\Theta}}_m\end{pmatrix}=\boldsymbol{J}_{sm}\dot{\boldsymbol{\Theta}}, \tag{4}$$

where $\boldsymbol{x}=\boldsymbol{h}(\boldsymbol{\Theta})\in\boldsymbol{R}^n$ is the pose of the end-effector of the manipulator in Cartesian space; $\boldsymbol{J}_s$ is the Jacobian matrix of the base; $\boldsymbol{J}_m$ is the Jacobian matrix of the actual manipulator; $\boldsymbol{I}$ is an identity matrix; $\boldsymbol{O}$ is a $6\times n$ zero matrix and $\boldsymbol{J}_{sm}\in\boldsymbol{R}^{m\times m}$ is the augmented Jacobian matrix of the system.

If $\boldsymbol{J}_m$ is non-singular, then from (4) we have:

$$\ddot{\boldsymbol{\Theta}}=\boldsymbol{J}_{sm}^{-1}\left(\ddot{\boldsymbol{X}}-\dot{\boldsymbol{J}}_{sm}\dot{\boldsymbol{\Theta}}\right). \tag{5}$$

Substituting (5) and $\dot{\boldsymbol{\Theta}}=\boldsymbol{J}_{sm}^{-1}\dot{\boldsymbol{X}}$ into the system-dynamic equation in joint space (3) and multiplying both sides of the equation by $\boldsymbol{J}_{sm}^{-\mathrm{T}}$, the dynamic equation in Cartesian space of the FFSR system can be obtained:

$$\boldsymbol{M}_a(\boldsymbol{\Theta})\ddot{\boldsymbol{X}}+\boldsymbol{B}_a(\boldsymbol{\Theta},\dot{\boldsymbol{\Theta}})\dot{\boldsymbol{X}}=\boldsymbol{J}_{sm}^{-\mathrm{T}}\begin{pmatrix}\boldsymbol{D}_s\\ \boldsymbol{\tau}+\boldsymbol{D}_m\end{pmatrix}, \tag{6}$$

where $\boldsymbol{M}_a=\boldsymbol{J}_{sm}^{-\mathrm{T}}\boldsymbol{\Omega}\boldsymbol{J}_{sm}^{-1}$, $\boldsymbol{B}_a=\boldsymbol{J}_{sm}^{-\mathrm{T}}\boldsymbol{K}\boldsymbol{J}_{sm}^{-1}-\boldsymbol{J}_{sm}^{-\mathrm{T}}\boldsymbol{\Omega}\boldsymbol{J}_{sm}^{-1}\dot{\boldsymbol{J}}_{sm}\boldsymbol{J}_{sm}^{-1}$.

To eliminate the base acceleration item, (6) can be written as the following two equations according to the partitioned matrix form:

$$\boldsymbol{M}_{mm}\ddot{\boldsymbol{x}}+\boldsymbol{M}_{ms}\ddot{\boldsymbol{\Theta}}_s+\boldsymbol{B}_{mm}\dot{\boldsymbol{x}}+\boldsymbol{B}_{ms}\dot{\boldsymbol{\Theta}}_s=\boldsymbol{J}_m^{-\mathrm{T}}(\boldsymbol{\tau}+\boldsymbol{D}_m), \tag{7}$$

$$\boldsymbol{M}_{sm}\ddot{\boldsymbol{x}}+\boldsymbol{M}_{ss}\ddot{\boldsymbol{\Theta}}_s+\boldsymbol{B}_{sm}\dot{\boldsymbol{x}}+\boldsymbol{B}_{ss}\dot{\boldsymbol{\Theta}}_s=\boldsymbol{D}_s-\boldsymbol{J}_s^{\mathrm{T}}\boldsymbol{J}_m^{-\mathrm{T}}(\boldsymbol{\tau}+\boldsymbol{D}_m). \tag{8}$$

where $\boldsymbol{M}_{mm}=\boldsymbol{T}_1\boldsymbol{T}_2$, $\boldsymbol{M}_{ms}=\boldsymbol{M}_{sm}^{\mathrm{T}}=\boldsymbol{T}_1\boldsymbol{T}_3$, $\boldsymbol{M}_{ss}=\boldsymbol{T}_3^{\mathrm{T}}\boldsymbol{\Omega}\boldsymbol{T}_3$; $\boldsymbol{B}_{mm}=\boldsymbol{T}_4\boldsymbol{T}_2-\boldsymbol{M}_{mm}\boldsymbol{T}_5$, $\boldsymbol{B}_{ms}=\boldsymbol{T}_4\boldsymbol{T}_3-\boldsymbol{M}_{mm}\dot{\boldsymbol{J}}\boldsymbol{T}_3$, $\boldsymbol{B}_{sm}=\boldsymbol{T}_3^{\mathrm{T}}\boldsymbol{K}\boldsymbol{T}_2-\boldsymbol{M}_{sm}\boldsymbol{T}_5$, $\boldsymbol{B}_{ss}=\boldsymbol{T}_3^{\mathrm{T}}\boldsymbol{K}\boldsymbol{T}_3-\boldsymbol{M}_{sm}\dot{\boldsymbol{J}}\boldsymbol{T}_3$; $\boldsymbol{T}_1=\boldsymbol{J}_m^{-\mathrm{T}}\begin{pmatrix}\boldsymbol{O}_{6\times m}\\ \boldsymbol{I}_{m\times m}\end{pmatrix}^{\mathrm{T}}\boldsymbol{\Omega}$, $\boldsymbol{T}_2=\begin{pmatrix}\boldsymbol{O}_{6\times m}\\ \boldsymbol{I}_{m\times m}\end{pmatrix}\boldsymbol{J}_m^{-1}$, $\boldsymbol{T}_3=\begin{pmatrix}\boldsymbol{I}_{6\times 6}\\ -\boldsymbol{J}_m^{-1}\boldsymbol{J}_s\end{pmatrix}$, $\boldsymbol{T}_4=\boldsymbol{J}_m^{-\mathrm{T}}\begin{pmatrix}\boldsymbol{O}_{6\times m}\\ \boldsymbol{I}_{m\times m}\end{pmatrix}^{\mathrm{T}}\boldsymbol{K}$, $\boldsymbol{T}_5=\dot{\boldsymbol{J}}_m\boldsymbol{J}_m^{-1}$; $\boldsymbol{M}$, $\boldsymbol{M}_{mm}$ and $\boldsymbol{M}_{ss}$ are symmetrical position matrices.

Resolving (7) and (8) simultaneously and removing $\ddot{\boldsymbol{\Theta}}_s$, we have the system-dynamic equation of the velocity and the acceleration of the end-effector in Cartesian space considering the external disturbances:

$$\boldsymbol{M}(\boldsymbol{\Theta})\ddot{\boldsymbol{x}}+\boldsymbol{B}(\boldsymbol{\Theta},\dot{\boldsymbol{\Theta}})\dot{\boldsymbol{x}}+\boldsymbol{G}(\boldsymbol{\Theta},\dot{\boldsymbol{\Theta}})=\boldsymbol{\tau}+\boldsymbol{D}_m-\boldsymbol{\Pi}\boldsymbol{M}_{ms}\boldsymbol{M}_{ss}^{-1}\boldsymbol{D}_s=\boldsymbol{\tau}+\boldsymbol{D}, \tag{9}$$

where $\boldsymbol{M}=\boldsymbol{\Pi}(\boldsymbol{M}_{mm}-\boldsymbol{M}_{ms}\boldsymbol{M}_{ss}^{-1}\boldsymbol{M}_{sm})$, $\boldsymbol{B}=\boldsymbol{\Pi}(\boldsymbol{B}_{mm}-\boldsymbol{M}_{ms}\boldsymbol{M}_{ss}^{-1}\boldsymbol{B}_{sm})$, $\boldsymbol{G}=\boldsymbol{\Pi}(\boldsymbol{B}_{ms}-\boldsymbol{M}_{ms}\boldsymbol{M}_{ss}^{-1}\boldsymbol{B}_{ss})\dot{\boldsymbol{\Theta}}_s$, $\boldsymbol{\Pi}=\boldsymbol{J}_m^{\mathrm{T}}(\boldsymbol{I}_{m\times m}+\boldsymbol{M}_{ms}\boldsymbol{M}_{ss}^{-1}\boldsymbol{J}_s^{\mathrm{T}})^{-1}$, $\boldsymbol{D}=\boldsymbol{D}_m-\boldsymbol{\Pi}\boldsymbol{M}_{ms}\boldsymbol{M}_{ss}^{-1}\boldsymbol{D}_s$.

3. Design of the robust adaptive controller

3.1 Basic robust adaptive controller

Define the position vector of the tracking error and the velocity vector of the tracking error as follows:

$$\begin{cases}\boldsymbol{e}=\boldsymbol{x}-\boldsymbol{x}_{\mathrm{d}},\\ \dot{\boldsymbol{e}}=\dot{\boldsymbol{x}}-\dot{\boldsymbol{x}}_{\mathrm{d}},\end{cases} \tag{10}$$

where $\boldsymbol{x}$ and $\dot{\boldsymbol{x}}$ represent the position and the velocity of the actual trajectory of the end-effector trajectory in Cartesian space, respectively and $\boldsymbol{x}_{\mathrm{d}}$ and $\dot{\boldsymbol{x}}_{\mathrm{d}}$ represent the position and the velocity of the desired trajectory of the end-effector in Cartesian space, respectively.

Define the reference velocity and the reference-acceleration vectors as follows:

$$\begin{cases}\dot{\boldsymbol{x}}_{\mathrm{r}}=\dot{\boldsymbol{x}}_{\mathrm{d}}-k\boldsymbol{e},\\ \ddot{\boldsymbol{x}}_{\mathrm{r}}=\ddot{\boldsymbol{x}}_{\mathrm{d}}-k\dot{\boldsymbol{e}},\end{cases} \tag{11}$$

where $\ddot{\boldsymbol{x}}_{\mathrm{d}}$ represents the acceleration of the desired trajectory of the end-effector in Cartesian space and k represents a positive constant.

Define the reference-tracking error and its velocity vector as follows:

$$\begin{cases}\boldsymbol{\eta}=\dot{\boldsymbol{x}}-\dot{\boldsymbol{x}}_r=\dot{\boldsymbol{e}}+k\boldsymbol{e},\\ \dot{\boldsymbol{\eta}}=\ddot{\boldsymbol{x}}-\ddot{\boldsymbol{x}}_r=\ddot{\boldsymbol{e}}+k\dot{\boldsymbol{e}},\end{cases} \tag{12}$$

where $\boldsymbol{\eta}$ and $\dot{\boldsymbol{\eta}}$ represent the reference-tracking error and its velocity vector, respectively.

Take one group of parameter initial values $\boldsymbol{\alpha}_0$ as the system's real parameter values. According to (9), the system's initial dynamic model is:

$$\boldsymbol{M}_0(\boldsymbol{\alpha}_0,\boldsymbol{\Theta}_0)\ddot{\boldsymbol{x}}+\boldsymbol{B}_0(\boldsymbol{\alpha}_0,\boldsymbol{\Theta}_0,\dot{\boldsymbol{\Theta}}_0)\dot{\boldsymbol{x}}+\boldsymbol{G}_0(\boldsymbol{\alpha}_0,\boldsymbol{\Theta}_0,\dot{\boldsymbol{\Theta}}_0)=\boldsymbol{\tau}_0. \tag{13}$$

where $\boldsymbol{M}_0$, $\boldsymbol{B}_0$ and $\boldsymbol{G}_0$ are coefficient matrices. $\boldsymbol{M}_0$ varies only with the variation of a joint's angle and velocity, and does not vary with the variation of the parameters to be identified. Thus, by selecting suitable initial parameters, $\boldsymbol{M}_0$ can be ensured so that it is easily and constantly invertible.

Inducing $\boldsymbol{\nu}$ into (13), the nominal controller can be obtained:

$$\boldsymbol{\tau}_0 = \boldsymbol{M}_0\boldsymbol{v} + \boldsymbol{B}_0\dot{\boldsymbol{x}} + \boldsymbol{G}_0. \tag{14}$$

Combining (9) and (14), we have $\boldsymbol{M}_0(\ddot{\boldsymbol{x}}-\boldsymbol{\nu})=\boldsymbol{0}$. If $\boldsymbol{M}_0$ is reversible, then $\ddot{\boldsymbol{x}}=\boldsymbol{\nu}$. If $\boldsymbol{\nu}=\ddot{\boldsymbol{x}}_r-k_s\boldsymbol{\eta}$, then the expression of the nominal controller can be obtained as:

$$\boldsymbol{\tau}_0 = \boldsymbol{M}_0(\ddot{\boldsymbol{x}}_r - k_s\boldsymbol{\eta}) + \boldsymbol{B}_0\dot{\boldsymbol{x}} + \boldsymbol{G}_0, \tag{15}$$

Design a robust adaptive controller as follows:

$$\boldsymbol{\tau} = \boldsymbol{M}_0(\ddot{\boldsymbol{x}}_r - k_s\boldsymbol{\eta}) + \boldsymbol{B}_0\dot{\boldsymbol{x}} + \boldsymbol{G}_0 + \boldsymbol{\tau}_u, \tag{16}$$

where $\boldsymbol{\tau}_u$ is the dynamic compensation part to be designed.

Select the compensation controller to be designed as:

$$\boldsymbol{\tau}_u = -\boldsymbol{W}\Delta\hat{\boldsymbol{\alpha}}, \tag{17}$$

where $\Delta\hat{\boldsymbol{\alpha}}=\boldsymbol{\alpha}_0-\hat{\boldsymbol{\alpha}}$, $\hat{\boldsymbol{\alpha}}$ is the estimate vector of $\boldsymbol{\alpha}$.

The torque prediction error is:

$$\sigma = \boldsymbol{W}\Delta\boldsymbol{\alpha} - \boldsymbol{W}\Delta\hat{\boldsymbol{\alpha}} = \boldsymbol{W}\tilde{\boldsymbol{\alpha}}. \tag{18}$$

The parameter-estimation law employs the torque-prediction error and the tracking error simultaneously to drive the parameter estimator; the compound parameter-estimation law is selected as follows:

$$\dot{\tilde{\boldsymbol{\alpha}}} = -\boldsymbol{\Gamma}^{-1}\boldsymbol{W}^{\mathrm{T}}\boldsymbol{\sigma} - \boldsymbol{\Gamma}^{-1}\boldsymbol{W}^{\mathrm{T}}\boldsymbol{M}_0^{-\mathrm{T}}\boldsymbol{\eta}. \tag{19}$$

where $\boldsymbol{\Gamma}$ represents the adaptive update rate that is a positive, definite diagonal-constant matrix.

3.2 Robustness analysis

$\boldsymbol{W}^{\mathrm{T}}\boldsymbol{W}$ is non-singular, and the boundary form of the external disturbance to the system is given, which can be described as:

$$\left\|\boldsymbol{D}\right\| = \left\|\boldsymbol{D}_m - \boldsymbol{\Pi}\boldsymbol{M}_{ms}\boldsymbol{M}_{ss}^{-1}\boldsymbol{D}_s\right\| \le \boldsymbol{D}_0 + \boldsymbol{D}_1\left\|\boldsymbol{\eta}\right\|, \tag{20}$$

where $\boldsymbol{D}_0$ and $\boldsymbol{D}_1$ are the known positive constants.

Combining (9) and (16), the closed-loop system with external disturbance is:

$$\dot{\boldsymbol{\eta}} + k_s\boldsymbol{\eta} = \boldsymbol{M}_0^{-1}(\boldsymbol{W}\Delta\boldsymbol{\alpha} + \boldsymbol{\tau}_u + \boldsymbol{D}_m - \boldsymbol{\Pi}\boldsymbol{M}_{ms}\boldsymbol{M}_{ss}^{-1}\boldsymbol{D}_s), \tag{21}$$

where $\Delta\boldsymbol{\alpha}=\boldsymbol{\alpha}_0-\boldsymbol{\alpha}$ is the difference vector between the parameter's initial values and the true values.

The following theorem, **Theorem 1,** is established considering the robust stability of the closed-loop system (21).

Theorem 1: Assuming that the external disturbance of the system is bounded, (19) is satisfied and $\boldsymbol{W}^{\mathrm{T}}\boldsymbol{W}$ is non-singular, then the control system shown in (19) and (21) is stable; that is, the parameters in the closed-loop system are bounded, and the reference-tracing error $\|\boldsymbol{\eta}\|$ and the parameter-estimation error $\|\tilde{\boldsymbol{\alpha}}\|$ are located in the ellipse as defined by the following inequation:

$$(\boldsymbol{C}_0 - \boldsymbol{C}_1\boldsymbol{D}_1)\left(\left\|\boldsymbol{\eta}\right\| - \frac{\boldsymbol{C}_1\boldsymbol{D}_0}{2(\boldsymbol{C}_0 - \boldsymbol{C}_1\boldsymbol{D}_1)}\right)^2 + \boldsymbol{C}_2\left\|\tilde{\boldsymbol{\alpha}}\right\|^2 \le \frac{\boldsymbol{C}_1^2\boldsymbol{D}_0^{\,2}}{4(\boldsymbol{C}_0 - \boldsymbol{C}_1\boldsymbol{D}_1)}, \tag{22}$$

where $\boldsymbol{C}_1$ is a constant defined as $\lambda_{\min}(\boldsymbol{M}_0^{-1})$; $\boldsymbol{C}_2$ is defined as $\lambda_{\min}(\boldsymbol{W}^{\mathrm{T}}\boldsymbol{W})$; $\boldsymbol{C}_0$ is defined as $\lambda_{\min}(k_s\boldsymbol{I})$ and $\lambda_{\min}(\bullet)$ represents the minimum singular value of $\bullet$.

Proof: the Lyapunov function is defined as:

$$V = \frac{1}{2}(\boldsymbol{\eta}^{\mathrm{T}}\boldsymbol{\eta} + \tilde{\boldsymbol{\alpha}}^{\mathrm{T}}\boldsymbol{\Gamma}\tilde{\boldsymbol{\alpha}}). \tag{23}$$

The time derivative of V is:

$$\begin{aligned}
\dot{V} &= \boldsymbol{\eta}^{\mathrm{T}}\dot{\boldsymbol{\eta}} + \tilde{\boldsymbol{\alpha}}^{\mathrm{T}}\boldsymbol{\Gamma}\dot{\tilde{\boldsymbol{\alpha}}} = \boldsymbol{\eta}^{\mathrm{T}}(\boldsymbol{M}_0^{-1}(\boldsymbol{W}\Delta\boldsymbol{\alpha}\text{-}\boldsymbol{W}\Delta\tilde{\boldsymbol{\alpha}} + \boldsymbol{D})\text{-}k_s\boldsymbol{\eta}) + \tilde{\boldsymbol{\alpha}}^{\mathrm{T}}\boldsymbol{\Gamma}\dot{\tilde{\boldsymbol{\alpha}}} \\
&= \boldsymbol{\eta}^{\mathrm{T}}\boldsymbol{M}_0^{-1}\boldsymbol{W}\tilde{\boldsymbol{\alpha}} + \boldsymbol{\eta}^{\mathrm{T}}\boldsymbol{M}_0^{-1}\boldsymbol{D}\text{-}\boldsymbol{\eta}^{\mathrm{T}}k_s\boldsymbol{\eta} - \tilde{\boldsymbol{\alpha}}^{\mathrm{T}}(\boldsymbol{W}^{\mathrm{T}}\boldsymbol{\sigma} + \boldsymbol{W}^{\mathrm{T}}\boldsymbol{M}_0^{-\mathrm{T}}\boldsymbol{\eta}) \\
&= \boldsymbol{\eta}^{\mathrm{T}}\boldsymbol{M}_0^{-1}\boldsymbol{D}\text{-}\boldsymbol{\eta}^{\mathrm{T}}k_s\boldsymbol{\eta} - \tilde{\boldsymbol{\alpha}}^{\mathrm{T}}\boldsymbol{W}^{\mathrm{T}}\boldsymbol{W}\tilde{\boldsymbol{\alpha}} \\
&\le C_1\left\|\boldsymbol{\eta}\right\|\left\|\boldsymbol{D}\right\| - C_0\left\|\boldsymbol{\eta}\right\|^2 - C_2\left\|\tilde{\boldsymbol{\alpha}}\right\|^2 \\
&\le C_1\left\|\boldsymbol{\eta}\right\|(D_0 + D_1\left\|\boldsymbol{\eta}\right\|) - C_0\left\|\boldsymbol{\eta}\right\|^2 - C_2\left\|\tilde{\boldsymbol{\alpha}}\right\|^2 \\
&\le -(\boldsymbol{C}_0 - \boldsymbol{C}_1\boldsymbol{D}_1)\left(\left\|\boldsymbol{\eta}\right\| - \frac{\boldsymbol{C}_1\boldsymbol{D}_0}{2(\boldsymbol{C}_0 - \boldsymbol{C}_1\boldsymbol{D}_1)}\right)^2 - \boldsymbol{C}_2\left\|\tilde{\boldsymbol{\alpha}}\right\|^2 + \frac{\boldsymbol{C}_1^2\boldsymbol{D}_0^{\,2}}{4(\boldsymbol{C}_0 - \boldsymbol{C}_1\boldsymbol{D}_1)},
\end{aligned} \tag{24}$$

According to the formula above, if $\boldsymbol{C}_0$ (i.e., k_s) is large enough to satisfy $\boldsymbol{C}_0-\boldsymbol{C}_1\boldsymbol{D}_1>0$, , then the right-hand side of the inequality (24) defines an ellipse in the two-dimensional space whose axes are $\|\boldsymbol{\eta}\|$ and $\|\tilde{\boldsymbol{\alpha}}\|$, and $\{\boldsymbol{\eta}, \boldsymbol{\sigma} \mid \dot{V}>0\}$ is satisfied in the ellipse. Thus, if $(\boldsymbol{\eta}, \tilde{\boldsymbol{\alpha}})$ is outside the ellipse, i.e., the reference-tracking error or parameter-estimation error exceed the limit defined by the ellipse, then $\dot{V}<0$, which means that $\boldsymbol{\eta}$ and $\tilde{\boldsymbol{\alpha}}$ are bounded. Therefore, the reference-tracking error and the parameter-estimation error will locate in the ellipse as defined by (22).

To illustrate that the tracking error is bounded, Lemma 1 is introduced.

Lemma 1: If $\|\boldsymbol{\eta}\| \le \zeta(\zeta<\infty)$ is satisfied for $t\in[t_0, \infty)$, and t_0 is a positive real number, then $\|e(t)\| \le \exp(-k(t-t_0))\left(\|e(t_0)\| - \frac{\zeta}{k}\right) + \frac{\zeta}{k}$, $\|\dot{e}(t)\| \le \zeta + k\|e(t)\|$ [24].

According to Lemma 1, the tracking error e and the velocity of the tracking error $\dot{e}$ are limited as $t \to \infty$.

4. Modification of the parameter-estimation law for robustness

4.1 The case of a known external-disturbance boundary form

The method proposed above needs $W^{\mathrm{T}}W$ to be non-singular, which is a strict condition. In this section, the modification of the parameter-estimation law is adopted to address the robustness issue when $W^{\mathrm{T}}W$ is singular. First, a convex compact set $Q(N)$ is defined as $Q(N)=\left\{\hat{\alpha} : \|\hat{\alpha}\| \le N\right\}$, where the positive constant N is a design parameter. In fact, the set defines a sphere whose radius is N, then N needs to be large enough to derive the truth values of the parameters to be estimated, which are located within the sphere, i.e., $\|\alpha\| \le N$.

The controller is the same as that denoted by (16), and the modified parameter-estimation law is: [25]

$$\dot{\hat{\alpha}} = -\Gamma^{-1}W^{\mathrm{T}}\sigma - \Gamma^{-1}W^{\mathrm{T}}M_0^{-\mathrm{T}}\eta - \Gamma^{-1}A, \tag{25}$$

$$A = \begin{cases} \hat{\alpha}\left(1-\dfrac{\|\hat{\alpha}\|}{N}\right)^2, & \|\hat{\alpha}\| > N, \\ 0, & \|\hat{\alpha}\| \le N. \end{cases} \tag{26}$$

The following theorem, **Theorem 2**, is established, considering the stability of the closed-loop system (21).

Theorem 2: If k_s is big enough and the parameter C_0 satisfies $C_0 - C_1D_1 > 0$, then the control system constructed by (21) and (25) is stable. That is, the variables in the loop are bounded, and the reference-tracking error $\|\eta\|$ and the torque-prediction error $\|\sigma\|$ are located in the ellipse defined by the following inequation:

$$(C_0 - C_1D_1)\left(\|\eta\| - \frac{C_1D_0}{2(C_0 - C_1D_1)}\right)^2 + \|\sigma\|^2 \le \frac{C_1^2D_0^{\,2}}{4(C_0 - C_1D_1)}, \tag{27}$$

where C_0 is defined as $\lambda_{\min}(k_s I)$, C_1 is a constant defined as $\lambda_{\min}(M_0^{-1})$ and $\lambda_{\min}(\bullet)$ represents the minimum singular value of $\bullet$.

Proof: The Lyapunov function is defined as:

$$V = \frac{1}{2}(\eta^{\mathrm{T}}\eta + \tilde{\alpha}^{\mathrm{T}}\Gamma\tilde{\alpha}). \tag{28}$$

The time derivative of V is:

$$\begin{aligned} \dot{V} &= \eta^{\mathrm{T}}\dot{\eta} + \tilde{\alpha}^{\mathrm{T}}\Gamma\dot{\tilde{\alpha}} = \eta^{\mathrm{T}}M_0^{-1}W\tilde{\alpha} + \eta^{\mathrm{T}}M_0^{-1}D - \eta^{\mathrm{T}}k_s\eta - \tilde{\alpha}^{\mathrm{T}}(W^{\mathrm{T}}\sigma + W^{\mathrm{T}}M_0^{-\mathrm{T}}\eta + A) \\ &= \eta^{\mathrm{T}}M_0^{-1}D - \eta^{\mathrm{T}}k_s\eta - \tilde{\alpha}^{\mathrm{T}}W^{\mathrm{T}}W\tilde{\alpha} - \tilde{\alpha}^{\mathrm{T}}A \\ &= \eta^{\mathrm{T}}M_0^{-1}D - \eta^{\mathrm{T}}k_s\eta - \sigma^{\mathrm{T}}\sigma - \tilde{\alpha}^{\mathrm{T}}A \\ &\le C_1\|\eta\|\|D\| - C_0\|\eta\|^2 - \|\sigma\|^2 - \tilde{\alpha}^{\mathrm{T}}A \\ &\le C_1\|\eta\|(D_0 + D_1\|\eta\|) - C_0\|\eta\|^2 - \|\sigma\|^2 - \tilde{\alpha}^{\mathrm{T}}A \\ &\le -(C_0 - C_1D_1)\left(\|\eta\| - \frac{C_1D_0}{2(C_0 - C_1D_1)}\right)^2 - \|\sigma\|^2 + \frac{C_1^2D_0^{\,2}}{4(C_0 - C_1D_1)} - \tilde{\alpha}^{\mathrm{T}}A. \end{aligned} \tag{29}$$

When $\|\hat{\alpha}\| > N$, the last item of (29) is:

$$\begin{aligned} \tilde{\alpha}^{\mathrm{T}}A &= (\hat{\alpha} - \alpha)^{\mathrm{T}}\hat{\alpha}\left(1 - \frac{\|\hat{\alpha}\|}{N}\right)^2 = \frac{\left(\|\hat{\alpha}\|^2 - \alpha^{\mathrm{T}}\hat{\alpha}\right)\left(N - \|\hat{\alpha}\|\right)^2}{N^2} \\ &\ge \frac{\left(\|\hat{\alpha}\|^2 - \|\alpha\|\|\hat{\alpha}\|\right)\left(N - \|\hat{\alpha}\|\right)^2}{\|\hat{\alpha}\|^2} \left(\because 0 < N < \|\hat{\alpha}\|, \alpha^{\mathrm{T}}\hat{\alpha} \le \|\alpha\|\|\hat{\alpha}\|\right) \\ &= \left(N - \|\hat{\alpha}\|\right)^2 - \frac{\|\alpha\|}{\|\hat{\alpha}\|}\left(N - \|\hat{\alpha}\|\right)^2 \\ &> 0 \left(\because \|\alpha\| \le N, \|\hat{\alpha}\| > N\right). \end{aligned} \tag{30}$$

Thus, $\dot{V}$ is negative due to $-\tilde{\alpha}^{\mathrm{T}}A$.

Due to the projection effect, the parameter-estimation value α is bounded. If $\|\hat{\alpha}\| \le N$, then $A = 0$. According to (29), if C_0 (i.e., k_s) is big enough and satisfies $C_0 - C_1D_1 > 0$, then the first three items on the right-hand side of the inequality (29) define an ellipse whose axes are $\|\eta\|$ and $\|\sigma\|$, and $\{\eta, \sigma \mid \dot{V} > 0\}$ is satisfied in the eclipse. Thus, if $(\eta, \tilde{\alpha})$ is not in the ellipse, the reference-tracking error or the torque-prediction error will finally be in the ellipse defined by (27).

According to Lemma 1, the tracking error e and the velocity of the tracking error $\dot{e}$ are bounded as $t \to \infty$.

4.2 The case of an unknown external-disturbance boundary form

Although the singularity problem of $W^{\mathrm{T}}W$ is solved in Section 4.1, the external-disturbance boundary form should be known. In this section, the σ_s modification method is adopted to modify the parameter-estimation law, which does not require the non-singularity of $W^{\mathrm{T}}W$ and the known external-disturbance boundary form; only the condition of the external disturbance being bounded is necessary.

The external disturbances to the base and the manipulator are considered in turn, and it is assumed that the external disturbances have upper bounds:

$$\begin{cases} \|D_s\| \le \bar{D}_s < \infty, \\ \|D_m\| \le \bar{D}_m < \infty, \end{cases} \tag{31}$$

where $\bar{D}_s$ and $\bar{D}_m$ are the upper bounds of the external disturbances to the base and the manipulator respectively.

The controller is the same as that denoted by (16). Amend the parameter-estimation law as: [26]

$$\dot{\hat{\boldsymbol{\alpha}}} = -\boldsymbol{\Gamma}^{-1}\boldsymbol{W}^{\mathrm{T}}\boldsymbol{\sigma} - \boldsymbol{\Gamma}^{-1}\boldsymbol{W}^{\mathrm{T}}\boldsymbol{M}_0^{-\mathrm{T}}\boldsymbol{\eta} - \sigma_s\boldsymbol{\Gamma}^{-1}\hat{\boldsymbol{\alpha}} \tag{32}$$

$$\sigma_s = \begin{cases} 0 & \|\hat{\boldsymbol{\alpha}}\| \le \bar{\boldsymbol{\alpha}}, \\ \dfrac{\mu\|\tilde{\boldsymbol{\alpha}}\|^2}{\|\tilde{\boldsymbol{\alpha}}\|^2 + \mu^2} & \|\hat{\boldsymbol{\alpha}}\| > \bar{\boldsymbol{\alpha}}, \end{cases} \tag{33}$$

where μ is a positive constant and $\bar{\boldsymbol{\alpha}}$ is a positive constant that represents the upper bound of the parameter's truth value. We have the following theorem for the stability of the closed-loop system (21).

Theorem 3: If the control parameter $\boldsymbol{C}_0$ (i.e., k_s) is large enough, then the control system composed of (21) and (32) is stable; that is, the variables in the loop are bounded. If $\|\hat{\boldsymbol{\alpha}}\| \le \bar{\boldsymbol{\alpha}}$, then the reference-tracking error $\|\boldsymbol{\eta}\|$ and the torque-prediction error $\|\boldsymbol{\sigma}\|$ locate in an ellipse as defined by the following inequation:

$$\frac{\boldsymbol{C}_0}{2}\|\boldsymbol{\eta}\|^2 + \|\boldsymbol{\sigma}\|^2 \le \frac{\boldsymbol{C}}{2\boldsymbol{C}_0}(\bar{\boldsymbol{D}}_s + \bar{\boldsymbol{D}}_m)^2. \tag{34}$$

If $\|\hat{\boldsymbol{\alpha}}\| > \bar{\boldsymbol{\alpha}}$, then the reference-tracking error $\|\boldsymbol{\eta}\|$ and the torque-prediction error $\|\boldsymbol{\sigma}\|$ locate in the following ellipse:

$$\frac{\boldsymbol{C}_0}{2}\|\boldsymbol{\eta}\|^2 + \|\boldsymbol{\sigma}\|^2 \le \frac{\boldsymbol{C}}{2\boldsymbol{C}_0}(\bar{\boldsymbol{D}}_s + \bar{\boldsymbol{D}}_m)^2 + \frac{1}{4}\sigma_s\left(\bar{\boldsymbol{\alpha}}\right)^2, \tag{35}$$

where $\boldsymbol{C}_0$ and $\boldsymbol{C}_1$ are the same as those in Theorem 1.

Proof: the Lyapunov function is chosen as:

$$V = \frac{1}{2}(\boldsymbol{\eta}^{\mathrm{T}}\boldsymbol{\eta} + \tilde{\boldsymbol{\alpha}}^{\mathrm{T}}\boldsymbol{\Gamma}\tilde{\boldsymbol{\alpha}}). \tag{36}$$

The time derivative of V is:

$$\begin{aligned}
\dot{V} &= \boldsymbol{\eta}^{\mathrm{T}}\dot{\boldsymbol{\eta}} + \tilde{\boldsymbol{\alpha}}^{\mathrm{T}}\boldsymbol{\Gamma}\dot{\tilde{\boldsymbol{\alpha}}} \\
&= \boldsymbol{\eta}^{\mathrm{T}}\boldsymbol{M}_0^{-1}\boldsymbol{W}\tilde{\boldsymbol{\alpha}} + \boldsymbol{\eta}^{\mathrm{T}}\boldsymbol{M}_0^{-1}\boldsymbol{D}_m - \boldsymbol{\eta}^{\mathrm{T}}k_s\boldsymbol{\eta} - \tilde{\boldsymbol{\alpha}}^{\mathrm{T}}(\boldsymbol{W}^{\mathrm{T}}\boldsymbol{\sigma} + \boldsymbol{W}^{\mathrm{T}}\boldsymbol{M}_0^{-\mathrm{T}}\boldsymbol{\eta} + \sigma_s\hat{\boldsymbol{\alpha}}) - \boldsymbol{\eta}^{\mathrm{T}}\boldsymbol{M}_0^{-1}\boldsymbol{\Pi}\boldsymbol{M}_{ms}\boldsymbol{M}_{ss}^{-1}\boldsymbol{D}_s \\
&= \boldsymbol{\eta}^{\mathrm{T}}\boldsymbol{M}_0^{-1}\boldsymbol{D}_m - \boldsymbol{\eta}^{\mathrm{T}}k_s\boldsymbol{\eta} - \sigma^{\mathrm{T}}\boldsymbol{\sigma} - \sigma_s\tilde{\boldsymbol{\alpha}}^{\mathrm{T}}\hat{\boldsymbol{\alpha}} - \boldsymbol{\eta}^{\mathrm{T}}\boldsymbol{M}_0^{-1}\boldsymbol{\Pi}\boldsymbol{M}_{ms}\boldsymbol{M}_{ss}^{-1}\boldsymbol{D}_s \\
&\le \boldsymbol{C}_1\|\boldsymbol{\eta}\|\bar{\boldsymbol{D}}_m - \boldsymbol{C}_0\|\boldsymbol{\eta}\|^2 - \|\boldsymbol{\sigma}\|^2 - \sigma_s\tilde{\boldsymbol{\alpha}}^{\mathrm{T}}\hat{\boldsymbol{\alpha}} - \boldsymbol{\eta}^{\mathrm{T}}\boldsymbol{M}_0^{-1}\boldsymbol{\Pi}\boldsymbol{M}_{ms}\boldsymbol{M}_{ss}^{-1}\boldsymbol{D}_s \\
&\le -\frac{\boldsymbol{C}_0}{2}\|\boldsymbol{\eta}\|^2 - \|\boldsymbol{\sigma}\|^2 - \sigma_s\tilde{\boldsymbol{\alpha}}^{\mathrm{T}}\hat{\boldsymbol{\alpha}} + \boldsymbol{C}_3\|\boldsymbol{\eta}\|\bar{\boldsymbol{D}}_m + \boldsymbol{C}_3\|\boldsymbol{\eta}\|\bar{\boldsymbol{D}}_s - \frac{\boldsymbol{C}_0}{2}\|\boldsymbol{\eta}\|^2 \\
&\le -\frac{\boldsymbol{C}_0}{2}\|\boldsymbol{\eta}\|^2 - \|\boldsymbol{\sigma}\|^2 - \sigma_s\tilde{\boldsymbol{\alpha}}^{\mathrm{T}}\hat{\boldsymbol{\alpha}} - \frac{\boldsymbol{C}_0}{2}\left(\|\boldsymbol{\eta}\| - \frac{\boldsymbol{C}}{\boldsymbol{C}_0}(\bar{\boldsymbol{D}}_s + \bar{\boldsymbol{D}}_m)\right)^2 + \frac{\boldsymbol{C}^2}{2\boldsymbol{C}_0}(\bar{\boldsymbol{D}}_s + \bar{\boldsymbol{D}}_m)^2.
\end{aligned} \tag{37}$$

If $\|\hat{\boldsymbol{\alpha}}\| \le \bar{\boldsymbol{\alpha}}$, σ_s=0 , then:

$$\dot{V} \le -\frac{\boldsymbol{C}_0}{2}\|\boldsymbol{\eta}\|^2 - \|\boldsymbol{\sigma}\|^2 + \frac{\boldsymbol{C}}{2\boldsymbol{C}_0}(\bar{\boldsymbol{D}}_s + \bar{\boldsymbol{D}}_m)^2. \tag{38}$$

If $\|\hat{\boldsymbol{\alpha}}\| > \bar{\boldsymbol{\alpha}}$, we have:

$$\begin{aligned}
\dot{V} &\le -\frac{\boldsymbol{C}_0}{2}\|\boldsymbol{\eta}\|^2 - \|\boldsymbol{\sigma}\|^2 - \sigma_s\tilde{\boldsymbol{\alpha}}^{\mathrm{T}}(\tilde{\boldsymbol{\alpha}} + \boldsymbol{\alpha}) + \frac{\boldsymbol{C}}{2\boldsymbol{C}_0}(\bar{\boldsymbol{D}}_s + \bar{\boldsymbol{D}}_m)^2 \\
&\le -\frac{\boldsymbol{C}_0}{2}\|\boldsymbol{\eta}\|^2 - \|\boldsymbol{\sigma}\|^2 - \sigma_s\|\tilde{\boldsymbol{\alpha}}\|^2 + \sigma_s\|\tilde{\boldsymbol{\alpha}}\|\|\boldsymbol{\alpha}\| + \frac{\boldsymbol{C}}{2\boldsymbol{C}_0}(\bar{\boldsymbol{D}}_s + \bar{\boldsymbol{D}}_m)^2 \\
&= -\frac{\boldsymbol{C}_0}{2}\|\boldsymbol{\eta}\|^2 - \|\boldsymbol{\sigma}\|^2 - \sigma_s\left(\|\tilde{\boldsymbol{\alpha}}\| - \frac{1}{2}\|\boldsymbol{\alpha}\|\right)^2 + \frac{1}{4}\sigma_s\|\boldsymbol{\alpha}\|^2 + \frac{\boldsymbol{C}}{2\boldsymbol{C}_0}(\bar{\boldsymbol{D}}_s + \bar{\boldsymbol{D}}_m)^2 \\
&\le -\frac{\boldsymbol{C}_0}{2}\|\boldsymbol{\eta}\|^2 - \|\boldsymbol{\sigma}\|^2 + \frac{\boldsymbol{C}}{2\boldsymbol{C}_0}(\bar{\boldsymbol{D}}_s + \bar{\boldsymbol{D}}_m)^2 + \frac{1}{4}\sigma_s(\bar{\boldsymbol{\alpha}})^2,
\end{aligned} \tag{39}$$

where C_3=$\|\boldsymbol{M}_0^{-1}\boldsymbol{\Pi}\boldsymbol{M}_{ms}\boldsymbol{M}_{ss}^{-1}\|$ and C=max(C_1, C_3) .

The design of σ_s should ensure that σ_s is constantly non-negative, which can make the reference-tracking error converge to zero without disturbances. Meanwhile, since σ_s is designed to be a convergence function, it can curb the parameter-drift phenomenon, and adjust the convergence value by changing the value of μ . According to the above inequations, if $\boldsymbol{C}_0$ (i.e., k_s) is large enough, the right-hand side of the inequality (37) defines an ellipse in a two-dimensional space whose axes are $\|\boldsymbol{\eta}\|$ and $\|\sigma\|$, and in the ellipse we have $\{\boldsymbol{\eta}, \sigma \mid \dot{V} > 0\}$. Thus, if $(\boldsymbol{\eta}, \sigma)$ is not in the ellipse — that is, if the norm of the reference-tracking error or the torque-prediction error exceeds the limit of the ellipse — we have $\dot{V} < 0$, which means that $\boldsymbol{\eta}$ and $\boldsymbol{\sigma}$ are bounded. Thus, the reference-tracking error and the torque-prediction error will finally locate within the ellipse defined by (34) or (35).

Further, according to Lemma 1, the tracking error $\boldsymbol{e}$ and its rate of change $\dot{\boldsymbol{e}}$ are bounded as $t \to \infty$.

5. Simulations

5.1 The simulation examples of the modified, robust adaptive control

A 2-DOF FFSR model shown in Fig.2 is taken as the simulation object, and $\boldsymbol{\alpha}$ is the separated parameter vector of the dynamic equation for the FFSR system and is chosen as $\boldsymbol{\alpha}$=$\begin{pmatrix} m_0 & m_1 & m_2 & I_0 & I_1 & I_2 & m_1b_1 & m_2b_2 \end{pmatrix}^{\mathrm{T}}$. The truth values of the actual parameters are shown in Table I, and the initial values of the parameters to be estimated are chosen as $\boldsymbol{\alpha}_0$=$(32 \quad 4 \quad 1.8 \quad 5.3 \quad 0.33 \quad 0.15 \quad 2 \quad 0.9)^{\mathrm{T}}$. The desired trajectory of the end-effector in Cartesian space is an anticlockwise circle trajectory. The simulation time is 6s and the adaptive update rate is $\boldsymbol{\Gamma}$=$\boldsymbol{diag}(0.1 \quad 0.1 \quad 0.1 \quad 4 \quad 0.2 \quad 0.1 \quad 0.2 \quad 0.2)$. The feedback gains are k=20, k_s=20.

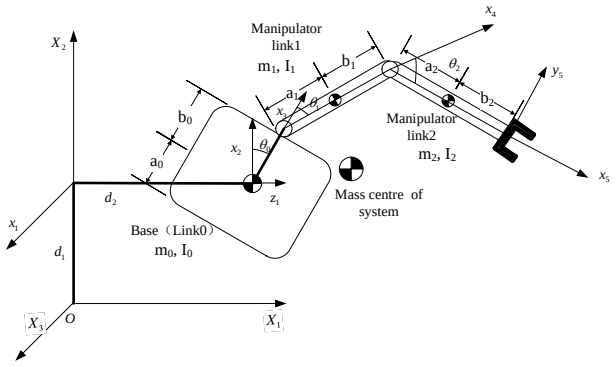

Figure 2. A 2-DOF FFSR model

link	a_i(m)	b_i(m)	m_i(kg)	I_i(kg · m^2)
0	0.5	0.5	80	40/3
1	0.5	0.5	8	2/3
2	0.5	0.5	6	1/2

Table 1. Parameters of 2-DOF FFSR system

To verify the robustness of the modified, robust adaptive controller, the simulation cases are divided into two types. One is the case of a known external-disturbance boundary form designed in Section 4.1 and the external disturbance is assumed to be $\boldsymbol{D}=(\boldsymbol{D}_s \ \boldsymbol{D}_m)^{\mathrm{T}}=$ $(0.3\sin 15t \ \ 0.2\cos 10t \ \ 0.5\sin 10t \ \ 0.4\sin 20t+0.3\theta_1 \ \ 0.2\cos 20t+0.3\theta_2)^T$, and $N=80$. The simulation results are shown in Fig. 3. The other case is that of an unknown external-disturbance boundary form designed in Section 4.2, where $\mu=0.1$ and the external disturbance is assumed to be $\boldsymbol{D}=(\boldsymbol{D}_s \ \ \boldsymbol{D}_m)^{\mathrm{T}}=$ $(0.3\sin 3t \ \ 0.2\cos 2t \ \ 0.5\sin 6t \ \ 0.4\sin 5t \ \ 0.2\cos 4t)^T$. The simulation results are shown in Fig. 4. Fig. 3(a) shows the error of an end-effector tracking-reference trajectory in Cartesian space with a known external-disturbance boundary form. Fig. 3(b) shows the actuation torques of Joint 1 and Joint 2 of the actual manipulator. Fig. 4(a) shows the error of the end-effector tracking reference trajectory in Cartesian space with an unknown external-disturbance boundary form. Fig. 4(b) shows the actuation torques of Joint 1 and Joint 2 of the actual manipulator. The simulation results show that under both conditions, the robust adaptive controller based on the modification of adaptive law can achieve robust stability and that the joint torques are realizable.

5.2 The simulation examples of the modified, robust adaptive control with practical disturbances

Take the FFSR system model above as the simulation object and examine the modified, robust adaptive controller with practical disturbances. The simulation time is 6s. In order to test the robustness of the controller further, the desired trajectory in the simulation is a line plus a semicircle. The manipulator is assumed to encounter an obstacle suddenly. At t=2s, the trajectory changes from the line to the semicircle, and the trajectory changes back to the original line from the semicircle at t=4s. The simulation cases are also divided into two types, and the external disturbances and parameter settings are the same as those of the two simulation cases discussed in Section 5.1. We also consider the non-linearities under practical conditions in the simulation [27], which include the measurement noise of the sensors and actuator saturation. The Gaussian noises have been introduced to the joint velocities, of which the mean is 0 rad/s and the variance is 7.6×10^{-7}. Gaussian noises have also been introduced to joint accelerations, of which the mean is 0 rad/s^2 and the variance is 7.6×10^{7}. The saturation condition for the actuator torque is added. The lower limit is -50 Nm and the upper limit is 50 Nm.

The simulation results are shown in Fig. 5 and Fig. 6. Compared with the simulation results in Section 5.1, the error of trajectory tracking fluctuates more obversely in Fig. 5(a) and Fig. 6(a), due to the amplification of the noise present in the measurements of joint velocities and accelerations. However, the robust adaptive controller designed in the paper can still track the desired trajectory stably, in spite of the practical disturbances affecting the overall

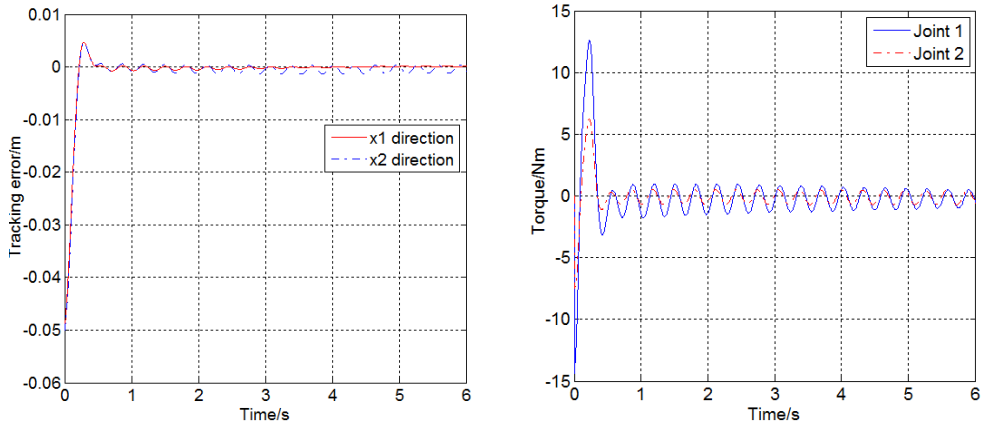

(a) Tracking errors (b) Joint torques of manipulator

Figure 3. The simulation case of a known external-disturbance boundary form

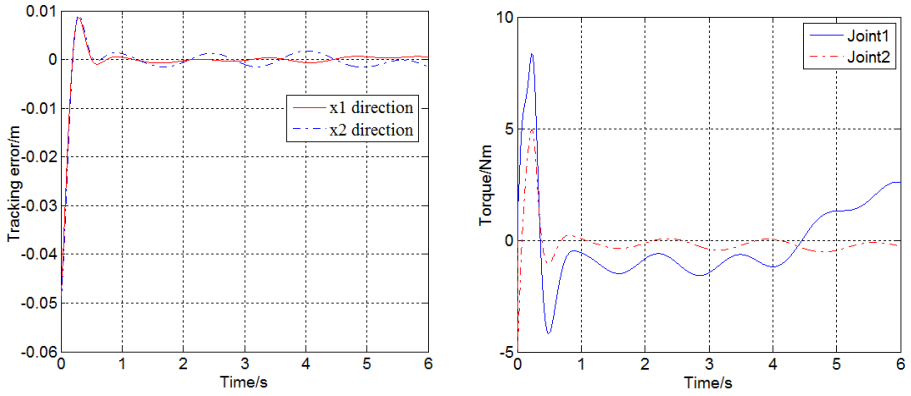

(a) Tracking errors (b) Joint torques of manipulator

Figure 4. The simulation case of an unknown external-disturbance boundary form

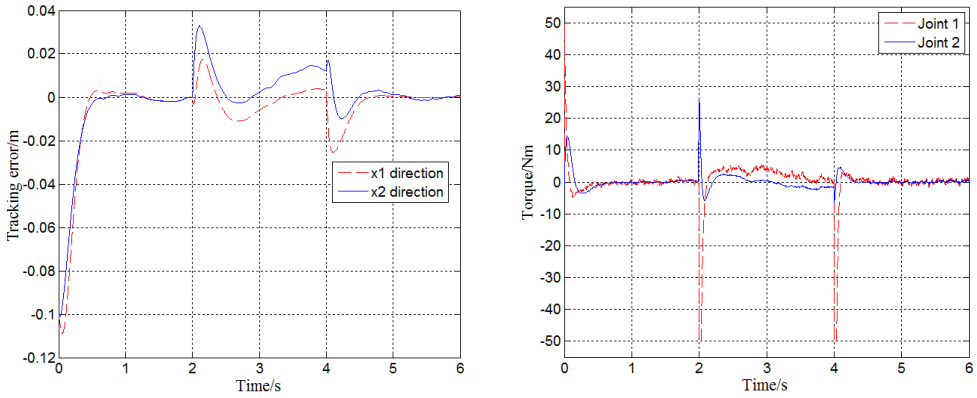

(a) Tracking errors (b) Joint torques of manipulator

Figure 5. The simulation case of a known external-disturbance boundary form, with noise and actuator saturation

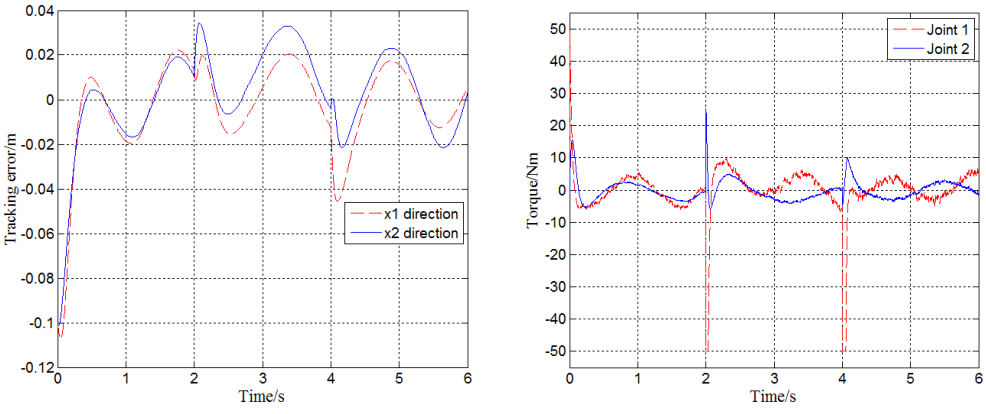

(a) Tracking errors (b) Joint torques of manipulator

Figure 6. The simulation case of an unknown external-disturbance boundary form, with noise and actuator saturation

closed-loop system. In Fig. 5(b) and Fig. 6(b), the input torques change suddenly at the inflexion points (t=2s and t=4s) of the desired trajectory, which leads to the condition of saturation. The saturation condition limits the actuator response to a reasonable extent, and the torques soon fall to the normal range under the control of the controller designed in the paper.

6. Conclusion

In the paper, a robust, adaptive trajectory-tracking strategy for the FFSR in Cartesian space is shown. By the modification of the parameter-estimation law, the control scheme can achieve robustness under conditions of known or unknown bounded-disturbance forms. The simulation

results demonstrate that the control scheme can ensure stable tracking of the desired trajectory of the end-effector of the FFSR in Cartesian space. Some practical conditions are also introduced, in which the system is affected by different types of disturbances, such as noise and actuator saturation. A good convergence is still presented in spite of the practical disturbances that affect the overall closed-loop system.

7. Acknowledgements

This work was supported by the National Natural Science Foundation of China (Grant No. 61203347), Self-Planned Task (NO. SKLRS201501C) of State Key Laboratory of Robotics and System (HIT), China Specialized Research Fund for the Doctoral Program of Higher Education (Grant No. 20122302120047), and the China Postdoctoral Science Foundation (Grant No. 2013M531023).

8. References

[1] Yoshida K, Hashizume K, Abiko S. Zero reaction maneuver: flight validation with ETS-VII space robot and extension to kinematically redundant arm. In: Proceedings of the IEEE International Conference on Robotics and Automation (ICRA'01); 21-26 May 2001; Seoul, Korea. New York: IEEE; 2001.p. 441–446.

[2] Flores-Abad A, Ma O, Pham K, et al. A review of space robotics technologies for on-orbit servicing. Progress in Aerospace Sciences. 2014; 68: 1–26.

[3] Fu Y, Zhang F, Wang S, et al. A dynamic control method for free-floating space manipulator in task space. In: Proceedings of the IEEE International Conference on Robotics and Biomimetics (ROBIO'07); 15-28 December 2007; Sanya, China. New York: IEEE; 2007. p. 1230–1235.

[4] Umetani Y, Yoshida K. Resolved motion rate control of space manipulators with generalized Jacobian matrix. IEEE Transactions on Robotics and Automation. 1989; 5: 303–314.

[5] Yoshida K, Kurazume R, Umetani Y. Torque optimization control in space robots with a redundant arm. In: Proceedings of the IEEE/RSJ International Workshop on Intelligence for Mechanical Systems (IROS'91); 3-5 November 1991; Osaka, Japan. New York: IEEE; 1991. p. 1647–1652.

[6] Torres S, Méndez J, Acosta L, et al. Efficient control of robot manipulators with model disturbances. In: Proceedings of the 45th IEEE Conference on Decision and Control (CDC'06); 13-15 December 2006; San Diego, USA. New York: IEEE; 2006. p. 2931–2936.

[7] Ehrenwald L, Guelman M. Integrated adaptive control of space manipulators. Journal of Guidance Control and Dynamics. 1998; 21: 156–163.

[8] Walker M. Adaptive control of space-based robot manipulators. IEEE Transactions on Robotics and Automation. 1992; 7: 828–835.

[9] Xu Y, Kanade T, Lee J. Parameterization control of space and adaptive robot system. IEEE Transactions on Aerospace and Electronic Systems. 1994; 30: 435–451.

[10] Gu Y, Xu Y. A normal form augmentation approach to adaptive control of space robot systems. Dynamics and Control. 1995; 5: 275–294.

[11] Parlaktuna O, Ozkan M. Adaptive control of free-floating space robots in Cartesian coordinates. Advanced Robotics. 2004; 18: 943–959.

[12] Parlaktuna O, Ozkan M. Adaptive control of free-floating space manipulators using dynamically equivalent manipulator model. Robotics and Autonomous Systems. 2004; 46: 185–193.

[13] Ortega R, Tang Y. Robustness of adaptive controllers — a survey. Automatica. 1989; 25: 651–677.

[14] Abdallah C, Dawson D, Dorato P, et al. Survey of robust control for rigid robots. IEEE Control Systems Magazine. 1991; 11: 24–30.

[15] Burkan R. Upper bounding estimation for robustness to the parameter uncertainty with trigonometric function in trajectory control of robot arms. Journal of Intelligent and Robotic Systems. 2006; 46: 263–283.

[16] Shin J, Jeong I, Lee J, et al. Adaptive robust control for free-flying space robots using norm-bounded property of uncertainty. In: Proceedings of the IEEE/RSJ International Conference on Intelligent Robots and Systems (IROS'95); 5-9 August 1995; Pittsburgh, USA. New York: IEEE; 1995. p. 59–64.

[17] Feng B, Ma G, Wen Q, et al. Adaptive robust control of space robot in task space. In: Proceedings of the IEEE International Conference on Mechatronics and Automation (ICMA'06); 25-28 June 2006; Luoyang, China. New York: IEEE; 2006.p. 1571–1576.

[18] Chu Z, Sun F, Cui J. Disturbance observer-based robust control of free-floating space manipulators. IEEE System Journal. 2008; 2: 114–119.

[19] Wang H. On adaptive inverse dynamics for free-floating space manipulators. Robotics and Autonomous Systems. 2011; 59: 782–788.

[20] Zhang W, Qi N, Ma J, et al. Neural integrated control for a free-floating space robot with suddenly changing parameters. Science China Information Sciences, 2011; 54: 2091–2099.

[21] Fang Y, Zhang W, Ye X. Variable Structure control for space robots based on neural networks. International Journal of Advanced Robotic Systems. 2014; 11: 1–7.

[22] Zhang W, Ye X, Jiang L, et al. Output feedback control for free-floating space robotic manipulators

base on adaptive fuzzy neural network. Aerospace Science and Technology. 2013; 29: 135–143.

[23] Wang H, Xie Y. On the recursive adaptive control for free-floating space manipulators. Journal of Intelligent & Robotic Systems. 2012; 66: 443–461.

[24] You S, Hall J. Model-based approach with adaptive bounds of robust controllers for robot manipulators. In: Proceedings of the IEEE International Conference on Systems, Man, and Cybernetics (SMC'94). 2-5 October 1994; San Antonio, TX, USA. New York: IEEE; 1994.p. 1279–1284.

[25] Feng G, Palaniswami M. Adaptive control of robot manipulators in task space. IEEE Transactions on Automatic Control. 1993; 38: 100–104.

[26] Reed J, Ioannou P. Instability analysis and robust adaptive control of robotic manipulators. In: Proceeding of the 27th IEEE International Conference on Decision and Control (CDC'88). 7-9 December 1988; Austin, TX, USA. New York: IEEE; 1988.p. 1607–1612.

[27] González-Vázquez S, Moreno-Valenzuela J. Motion control of a quadrotor aircraft via singular perturbations. International Journal of Advanced Robotic Systems. 2013; 10: 1–16.